Journal of Applied Polymer Science

Polyvinyl Chloride Composites Filled with Olive Stone Flour: Mechanical, Thermal, and Water Absorption Properties

Ilhem Naghmouchi,[1] Pere Mutjé,[2] Sami Boufi[1]
[1]Faculty of Science, University of Sfax, LMSE-3000 Sfax, Tunisia
[2]Department of Chemical Engineering, Group LEPAMAP, University of Girona, Girona 17071, Spain
Correspondence to: S. Boufi (E-mail: Sami.Boufi@fss.rnu.tn)

ABSTRACT: The production of olive oil leads to considerable amounts of solid waste mainly composed of hard woody endocarp called olive stones. The aim of this work is to explore the possible use of ground olive stones as fillers for polyvinyl chloride (PVC), to elaborate a cost-effective composite material with a solid loading of up to 50 wt %. After grinding, the ensuing olive stone flour (OSF) was incorporated into a PVC matrix via melt compounding and injection molding to elaborate PVC-OSF-based composites with a filler content up to 50 wt %. The evolution of the mechanical performance, the impact property, the water absorbance, and wear resistance behavior, according to the OSF content, were investigated. The addition of OSF was shown to enhance the stiffness of the matrix, but at the expense of its mechanical strength. However, the strength of the composite did not fall as low as 30 MPa, and therefore, meets the requirements for many applications in plastic-based materials. The thermal properties of the ensuing composites were also studied by thermogravimetric analysis. The results show that the addition of OSF may be effective in increasing the stiffness of the PVC-based composite and in reducing the solid residue in the olive oil industry production. © 2014 Wiley Periodicals, Inc. J. Appl. Polym. Sci. **2014**, *131*, 41083.

KEYWORDS: agricultural by product; composites; mechanical properties; olive

Received 16 March 2014; accepted 30 May 2014
DOI: 10.1002/app.41083

INTRODUCTION

Spain, Greece, Italy, Tunisia, and Turkey are the most important olive oil producers in the Mediterranean basin representing about 95% of the world production.[1] Tunisia is a leading olive oil producer, with over 65 million olive trees grown on 1.7 million hectares and an average annual production amounting to 200×10^3 T. The undeniable nutritional merits of olive oil are well-known; thus, the increasingly demand for it. However, the extraction process generates an "aqueous sludge" and a solid residue called "olive cake," which is obtained after extracting the oil from the fruit. Currently, from 100 kg of olives, about 20% of oil is recovered, and 30% of olive cake and about 50% of aqueous liquor generated. Due to their high phenolic content, the latter two fractions are not easily degradable by natural processes, and their disposal creates a major environmental issue in the main olive-producing countries. Accordingly, research into finding new possible uses for olive industry by-products, particularly the solid ones, is of a great relevance not only to the economy but also to the environment in these countries.

Different strategies have been reported in the literature to valorize the solid by-products generated by the olive oil extraction, to reduce the negative environmental impact. The solid waste can be burned to produce electric energy or heat,[2] or turned into activated carbon[3] after a thermal treatment for the removal of poisonous metals from water.[4] The possible use of the solid by-products as a source of compost material has also been approached.[5–11] The conversion of olive stone flour (OSF) into viscous polyols, likely to be used in polyurethane foams, was successfully accomplished by total and partial oxypropylation.[12] The use of the ground solid waste as a sustainable filler in polymer-based composite also constitutes an interesting potential application within the field of materials technology. In fact, given the high hardness of the olive stones, an enhancement in the stiffness of the polymer when the ground olive stone residue is incorporated within thermoplastic polymer matrix, might be expected. Although wood flour remains the main lignocellulosic filler[13,14] among the natural reinforcements, the use of agricultural by-products as a source of renewable filler or reinforcement in the production of plastic composites alleviates the shortage of wood resources, thus constituting an interesting alternative for making a bio-based composite. Despite the considerable amount of solid waste generated by olive oil extraction, to the best of our knowledge, only a few research works

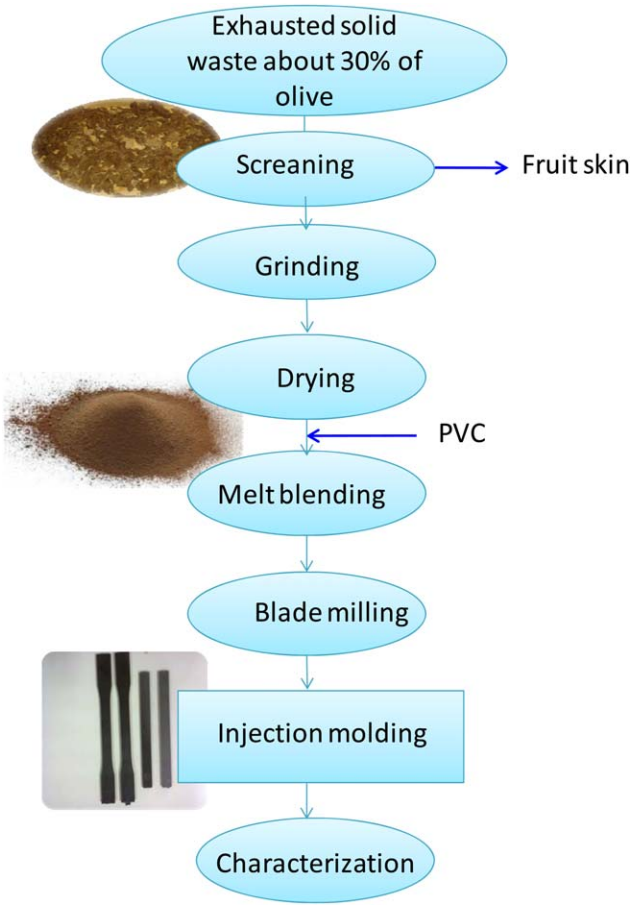

Figure 1. Process flow chart showing the processing route for SFO-based composite. [Color figure can be viewed in the online issue, which is available at wileyonlinelibrary.com.]

reported in the literature have tackled the use of olive stones as fillers in polymer-based composite materials. Using the search term "olive stone," "olive kernel," or "olive pit" and composites, only eight English scientific publications have been reported by ISI since 1993, six of which were devoted to thermoplastic matrix.[5–11] Among these reported research works, only two were concerned with polyvinyl chloride (PVC) as a polymer matrix.[12,15] However, the filler content has been limited to 25 wt %, and the characteristics of the used olive pomace, in terms of morphological and chemical composition, was not provided.

The purpose of this work is to investigate the effect of the incorporation of the OSF up to 50 wt % loading in PVC, on the tensile properties, flexural properties, impact strength, thermal properties, together with abrasion resistance. The OSF was prepared from exhausted solid olive oil mills after solvent extraction to further extract the pomace olive oil. After the drying and screening ventilation to separate the shell from the stone, the latter was dry ground to produce OSF. Although, the use of olive solid waste as a filler in the PVC matrix was the subject of two publications,[12,16] the novelty of this work compared to previous one is that, (i) only the hard endocarp stone, exempt from any residual oil and soft epicard, is used as a filler after grinding (ii), a wider filler loading up to 50 wt % was studied in this work, which is the common loading to produce cost-effective composite, and finally, (iii) the composites were processed using injection molding which imparts better filler homogeneity.

EXPERIMENTAL

Materials

The polymer matrix used in this study was PVC (SABIC-PVC 59S *K*-value 59). All formulations were prepared by adding 4 phr of Stabilox CZ 2973 GN, 3 phr of epoxydized soya bean oil, 0.5 phr of sodium stearate, and calcium stearate as lubricants (% based on solid PVC).

OSF Preparation

Olive stones flour used as a filler of PVC composites were produced from the solid residues of olive oil. After extracting the olive oil, there remained a residue of pulp and stone mixed with water. Water was evaporated and the solid residue extracted with hexane to recover the remaining oil. After drying, the solid residue was separated into shells and stones by screening ventilation. The stone, called the woody endocarp, represents about 18–25% of the olive weight (Figure 1) and is mainly composed of lignin, hemicellulose, and cellulose. The stone residue was ground to about a 200 μm average particle size.

Filler Characterization

The biomass used in this study consisted of olive stones crushed and sieved to obtain finer particles, from 50 to 400 μm in size.

Chemical Composition. The chemical composition of the dried fibers was determined according to TAPPI T 264 om-88 (TAPPI, 1988a). The samples were first submitted to Soxhlet extraction with ethanol/toluene and water, and then ash (Tappi T 211 om-93, 2000), extractive (Tappi T204 cm-07, 2007), Klason lignin (Tappi T222 om-83, 1999), and hemicellulose (Tappi T249-cm-85, 1999) contents were determined.

Particle Size. The length and aspect ratio of OSF filler was determined by Morfi analyses using TECHPAP LB 01 Morfi equipment (fiber content of 0.300 g/L).

Preparation of the Composite

OSF was dried in an oven under vacuum at 80°C overnight, to reduce the humidity content. A Gelimat thermokinetic mixer (a high-intensity turbine mixer) was used to mix the OSF filler with the PVC matrix. The compounding time in the Gelimat was about 100–150 s and a final mixing temperature of 190°C. The compounding temperature was varied and optimized not only to obtain an easily-processable homogeneous mixture but also to avoid the degradation of one of the constituents. The obtained composite blends were, then, pelletized into lengths of about 10 mm using a blade mill from AGRIMSA. Afterward, they were molded using an injection-molding machine (40-Mateu&Soler) to obtain specimens for tensile, three-point bend and impact tests. The machine is equipped with three heating areas working at 165, 175, and 190°C, the highest of which corresponds to the nozzle. The used steel mold was dimensioned

according to the ASTM D3641 standard. The processing route of the PVC/OSF composites is depicted in Figure 1. The specimens were conditioned according to the ASTM D618 standard before testing (23°C and 50% relative humidity for 3 days).

In the following the OSF content is designed as *X* wt %, where *X* represent the filler loading in 100 g of the composite.

Mechanical Characterization

Processed materials were analyzed after 48 h in a conditioning chamber (Dycometal) at (23 ± 3)°C and (50 ± 5)% relative humidity according to ASTM D638 standard specifications. The measurements of the specimens were, then, carried out using an INSTRON testing machine equipped with an extensometer. Tensile strength measurements and three-point bending tests were carried out following ASTM D638 and ASTM D790 standard methods, respectively. Five specimens were tested for each batch. The notched Charpy impact strength was measured according to ASTM D6110 using a Zess apparatus provided with a hammer of 2.074 kg in weight and 382 mm in arm length. The final results were given as the average of at least five samples.

Scanning Electron Microscopy

Scanning electron microscopy (SEM) was performed with a Zeiss DMS 960 SEM microscope operating at 25 kV. The specimens were carried out under liquid nitrogen not only to impede the plastic deformation of the matrix but also to get well-defined fiber-matrix interface prior to analysis. They were coated with a 10 nm layer of gold to avoid sample charging under the electron beam.

Thermal Behavior

The thermogravimetric analysis (TGA) was performed with STARe SW 9.2 thermogravimetric analyser. A sample of about 10 mg was used and a heating cycle from 20 to 600°C at a heating rate of 10°C/min under oxygen atmosphere.

The differential scanning calorimetric (DSC) measurements were carried out with a DSC Q2000 V24.4 Build 116 at a heating rate of 10°C/min in a nitrogen atmosphere with a gas flow of 30 mL/min. Each thermogram was registered from 20° to 160°C to rub out the previous thermal history of PVC fiber to estimate the glass transition temperatures T_g. The samples were, then, cooled down to 20°C at 10°C/min and, subsequently, the composites charged with different percentages were heated to 160°C at 10°C/min in the second scan.

Moisture content

The samples were immersed in distilled water at room temperature, that is, 25°C. After specific time intervals, the samples were removed from water. Next, their surface moisture was removed by tissue paper, weighed in a high precision balance to find the amount of water taken up and, then, submerged again in water. Moisture absorption was determined by the weight gain relative to the dry weight of the samples. The moisture content of a sample was computed as follows:

$$M_t = \left(\frac{W_t - W_0}{W_0}\right) 100$$

where W_0 and W_t denote the dry weight of the sample and the weight at any specific time t, respectively.

Wear Resistance

The wear resistances were investigated using the Taber abrasion tester, according to ASTM D4060-10. A set of two rotating abrasive wheels with a diameter of 50 mm and a thickness of 12.6 mm was run against the specimens with dimensions 120 × 120 × 3 mm^3 at a contact load of 1000 g. The test was done for 1000 cycles and the wear resistance of the sample determined by measuring the specimen weight loss.

X-ray Diffraction Analysis

The crystalline degree of cellulose was calculated from an X-ray diffraction profile. X-ray measurements were made on SFO using Cu Kα radiation, generated with a Bruker AXS diffractometer (Bruker AXS, Madison, WI at 30 kV, 100 mA. Sweeps of 5–50° 2θ were made with a step size of 0.05 s and step time measurement of 10 s. The crystalline index (CrI) was calculated using the diffraction intensities of the crystalline structure and that of the amorphous fraction according to the method of Segal[16]

$$\text{CrI}\,\% = \left[\frac{I_{002} - I_{\text{am}}}{I_{002}}\right] 100$$

where I_{002} is the intensity of the crystalline peak at the maximum at 2θ between 22° and 23° for cellulose, and I_{am} is the intensity at the minimum at 2θ between 18° and 19° for cellulose.

RESULTS AND DISCUSSION

Characterization of OSF

SEM observation was conducted to explore the morphological characteristics in terms of size, aspect, and topography of the OSF. The observation at three levels of magnification (Figure 2) has revealed individualized compact particles with a broad distribution in size ranging from about 20 to 150 μm. Indeed, the shape of the particles is not uniform and seems to encompass mainly two populations, the first of which exhibits a granular form with a low particle size (lower than 50 μm) while the second includes acicular particles with an aspect ratio in the range of 4–10.

The chemical composition of OSF, given in Table I, confirms the lignocellulosic character of the filler as being composed of lignin, hemicelluloses cellulose, and extractives with contents of about 35%, 35,% 25%, and 5%, respectively. The bulk density of OSF particles is 1.2, which is quite lower than that of lignocellulosic fibers in the range of 1.5–1.6.[17] This low value may be the consequence of the low cellulose content of the material compared to that of lignocellulosic fibers. This lower bulk density may bring advantageous with regard to the weight gain in the composite materials.

The wide angle X-ray diffraction characterization of the OSF has revealed the presence of the main characteristic peaks of cellulose I at $2\theta = 22.6°$ and 15°, assigned to the [0 0 2] and [1 0 1] lattice plane, respectively. The crystalline index calculated

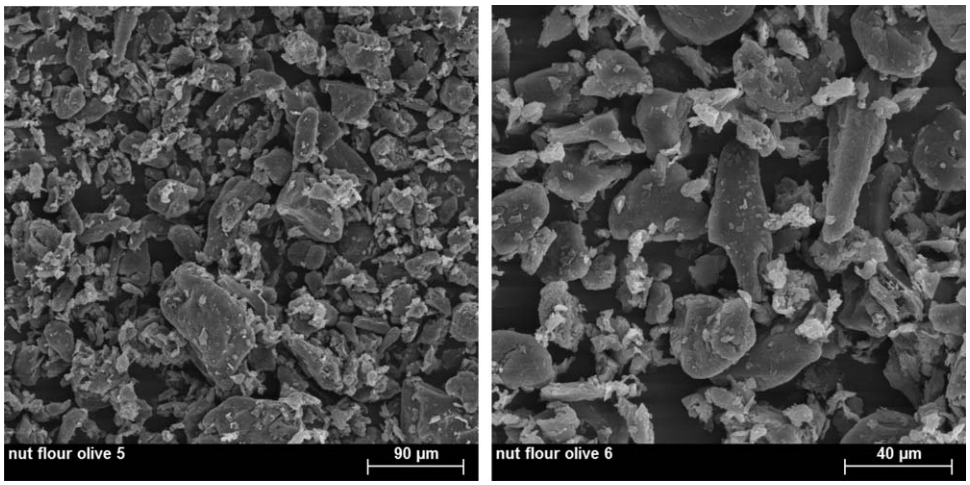

Figure 2. SEM micrograph showing the particle characteristics of the OSF used in the study.

according to the Segal method is about 35%, which is consistent with the low content of cellulose within OSF particles.

Evolution of the Mechanical Properties with OSF Loading

To investigate the effect of the OSF incorporation on the mechanical properties of PVC-based composites, composite samples with OSF content up to 50 wt % were prepared by internal blending followed by injection molding. Their mechanical performance in terms of the tensile strength, flexural strength, and impact resistance was also examined.

As can be seen in Figure 3(a), over the whole studied OSF contents, Young's and the flexural modulus increased linearly with the filler content as it was strongly affected by the characteristics of the incorporated filler and less affected by the polymer-filler adhesion. This trend is presumably the consequence of the higher stiffness of the OSF filler rather than that of the PVC matrix. The data for the composite tensile modulus in Figure 1 can be modeled using a number of approaches. One common approach is to use the Hirsch model[18] which is based on a combination of parallel and series rule-of-mixture models and was shown to be quite accurate for the estimation of the composite modulus with randomly distributed fiber.[19] It can be fitted with the following eq. (1):

$$E_t^c = \beta(E_t^F V^F + E_t^m(1-V^F)) + (1-\beta)\frac{E_t^F E_t^m}{E_t^m V^F + E_t^F(1-V^F)} \quad (1)$$

where β is the efficiency stress transfer factor between fiber and matrix, E_t is the Young's modulus, and V the volume fraction; c, m, and F refer to composite, matrix, and fiber, respectively. Based on our previous work,[13] it was shown that the β value around 0.4 for short lignocellulosic fibers correctly fits the experimental data. Adopting the Hirsh model, and a β value equal to 0.4, it was possible to estimate the intrinsic Young's modulus of OSF to 10.5 GPa by adjusting the E_f value to obtain the higher correlation.

Different behaviors are noted for tensile and flexural strength. As shown in Figure 3(b), both tensile and flexural strengths decreased with the increase in the content of the OSF. At 50% OSF content, the decrease in the tensile and flexural strengths reached about 30% and 38%, respectively, with respect to the unfilled matrix. A similar tendency has also been reported for PVC/wood flour composites,[20] which is likely the consequence of the lack of efficient interfacial adhesion between the filler and the PVC matrix.[21] However, one should note that the most apparent drop in the strength occurred at 20% OSF content and did not undergo further decrease with increasing in the OSF content over 20%. This behavior is different from that observed for a more hydrophobic matrix, such as polypropylene (PP) or polyethylene (PE), where a steady drop in the strength is observed when the lignocelluloseic filler is introduced without a coupling agent.[13] In fact, presently, given the quite polar character of PVC, one should expect polar–polar interaction between the polymer matrix and the OSF filler to occur. This was also observed in microcrystalline cellulose from waste cotton fabrics and PVA matrix.[22] The drop in the strength observed would be the consequence of the low aspect ratio of the OSF particles causing them to act as a stress concentrator rather than reinforcing filler. Actually, in short-fiber composites, there is a critical fiber length (L_c) below which the stress transfer from matrix to fibers is not enough to reach the fiber

Table I. The Chemical Composition and Physical Characteristics of OSF Used

Constituent	Amount
Ash[a]	5 ± 0.5%
Moisture content	7 ± 0.5%
Extractible	1.5 ± 0.3%
Hemicellulose	35 ± 2%
Cellulose	25 ± 3%
Holocellulose	60 ± 2%
Lignin	35 ± 2%
CrI(%)	35 ± 2%
Average particle size* (µm)	125 ± 50
Aspect ratio	4.4 ± 2
Density	1.2 ± 0.1

[a] Determined from Morfi analysis.

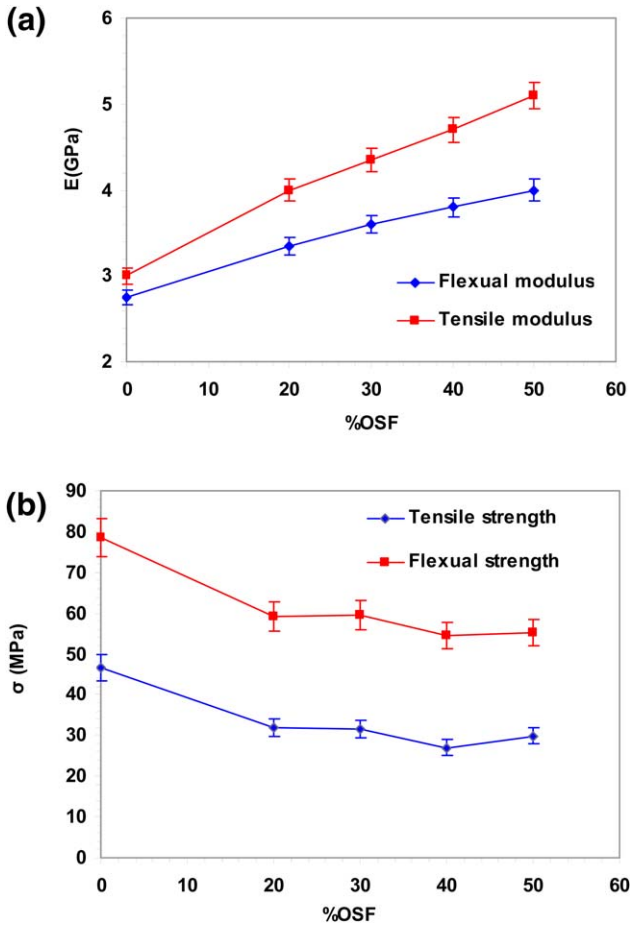

Figure 3. Evolution of (a) the tensile and flexural modulus and (b) the tensile and flexural strength versus OSF content. [Color figure can be viewed in the online issue, which is available at wileyonlinelibrary.com.]

fracture strength and the filler is underexploited. Although dependent on the interfacial quality and the strength properties of the filler, the value of L_c is often higher than 300 μm.[14,21] The quality of the interfacial adhesion between the OSF filler and the PVC matrix was assessed by SEM observation (Figure 4) where both zones of good and weak interfacial adhesion can be seen. However, it is worth noting that the mechanical strength of the composite did not fall as low as 30 MPa, and accordingly met the requirements for many applications in plastic-based materials.[23]

In composite-based material, a lower tensile strength property compared to that of the flexural strength is commonly observed.[24] Among the arguments given to explain this discrepancy, one can cite the difference in the stress distribution within the specimen in tensile and bending test. In the former, the stress distribution is fairly homogeneous (only tensile stress is present) whereas in the later, both tensile and compressive stresses are present and, in composite-based materials compressive properties is often higher than tensile ones. Another reason is associated to the presence of defects in the material acting as stress concentrator that generate localized weakness. As larger volume of material is tested in tensile test than in bending, then the presence of these weak zones favored premature breaking in the tensile stress.

The evolution in the impact strength of the composite following the OSF addition was also studied using a Charpy impact tester. The results shown in Figure 5 indicate an important reduction in both untouched and notched Charpy impact strengths on the addition of the filler, but with less effect for the notched samples. The decrease in the impact strength in the composite is expected as the stiff particles' filler act as stress concentrators in the polymer matrix, which in turn reduced the crack initiation energy and led to earlier interfacial debonding between the

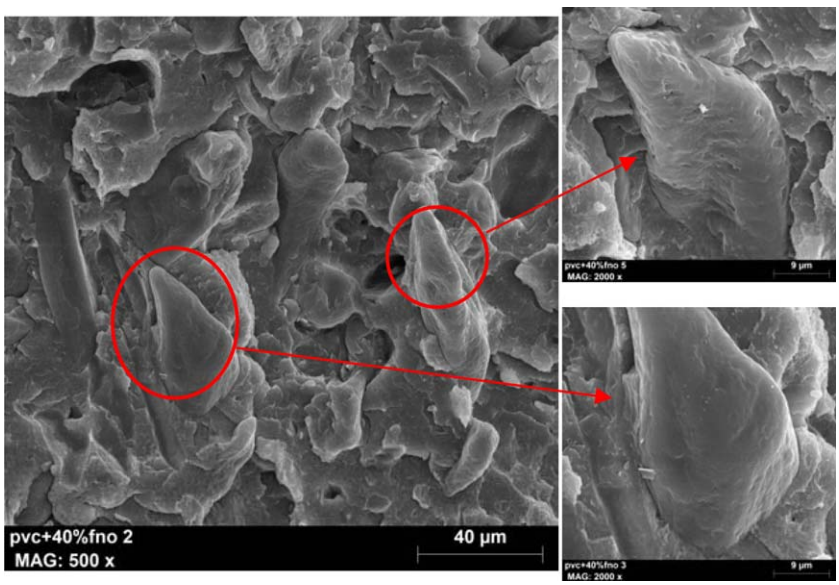

Figure 4. SEM micrograph of the tensile fractured surface for OSF-PVC composite. [Color figure can be viewed in the online issue, which is available at wileyonlinelibrary.com.]

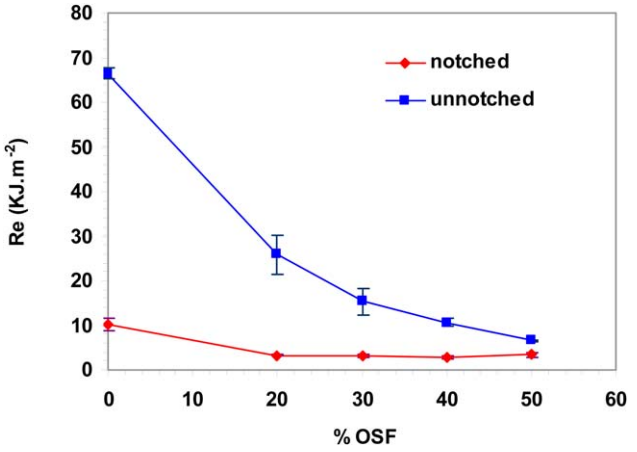

Figure 5. Evolution of the Charpy impact strength (a) untouched and (b) notched as a function of the OSF loading. [Color figure can be viewed in the online issue, which is available at wileyonlinelibrary.com.]

filler and the matrix. Conversely, once the crack is initiated, the OSF particles hamper its propagation by dissipating the energy through different mechanisms such as the filler-matrix interfacial debonding between the fiber and the matrix. This can explain the less sensitivity of the notched Charpy impact strength to the filler addition.

The addition of OSF to the PVC matrix brought about a continuous drop in the elongation at break. This effect is expected if we consider that the filler incorporation imparts rigidity and restrains the deformation on the matrix that leads to an inevitable decrease in the degree of the material ductility.

Wear Resistance

The use of a PVC lignocellulosic filler-based composite is increasingly popular in a wide range of applications; including composite decking, floor covering materials in buildings, and on wharf watersides. For all of these applications, wear is an important characteristic and should be analyzed in addition to the mechanical properties. The effect of the OSF addition on the wear behavior of PVC-OSF composites was assessed using the Taber abraser test by measuring the weight loss after 1000 cycles. Results in Figure 6 showed a steady increase in the weight loss versus the OSF loading up to a filler loading of 40% and then grew more steeply at 50% OSF. Weight loss increased by about 50% with respect to the unfilled matrix at a filler loading of 40% and grew by about 95% as the OSF content reached 50%. The decrease in the wear resistance might be explained by the increase in the stiffness of the composite as OSF filler is added to the PVC matrix. However, the deviation from linearity over 40% filler content is likely the result of the increased surface roughness resulting from the protrusion of the OSF particles as clearly shown in the SEM observation of the surface at different filler contents (see inset in Figure 6).

Water Absorption Properties

The most serious impediment related to the use of lignocellulosic filler in composite materials is its high sensitivity to water, which adversely affects its mechanical performance as well as its long term durability, particularly for outdoor use. The higher

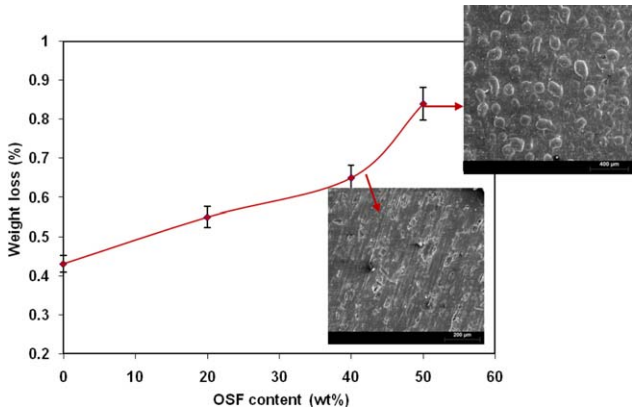

Figure 6. Wear weight loss versus OSF content. The inset shows the SEM observation of the surface at 30% and 50% OSF. [Color figure can be viewed in the online issue, which is available at wileyonlinelibrary.com.]

sensitivity of the composite based on lignocellulosic filler is the consequence of the inherent hydrophilic character of the filler, as well as the defects, such as voids, pores, and cracks at the interfacial zone filler/matrix, whose presence is likely to favor the diffusion and the accumulation of water within the composite through capillary effect. Furthermore, the possible contact between the OSF particles as their content exceeds a critical threshold is another parameter likely to contribute to water uptake through the creation of a percolating path for the water transport by capillarity through the filler network.[25]

Water uptake under immersion condition in the composites, as a function of exposure time and for different OSF loadings, is shown in Figure 7. The water content M_t rapidly increased at the first stage of absorption and, then, gradually slowed down until a saturation plateau is reached after about 1 month of immersion in water. It can be observed that the equilibrium water uptake increased with OSF content, which is in agreement with results noted for wood-based lignocellulosic fibers.[26]

The equilibrium uptake values of composites with different filler loadings are given in Figure 8. It is clear that M_∞ values increased with filler content, in a linear way. However, it is

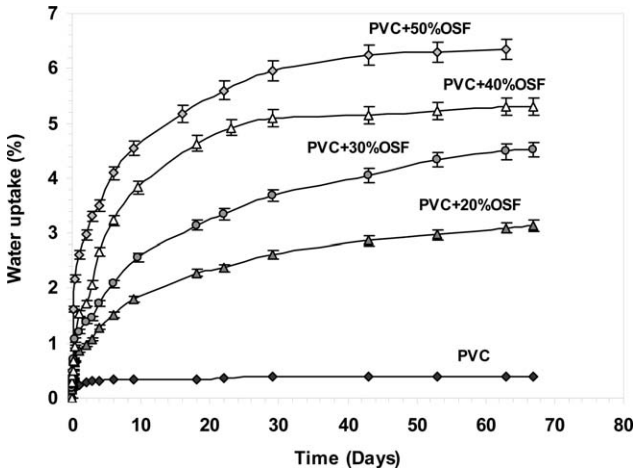

Figure 7. Water absorption behavior of composites with different filler loadings under immersion condition.

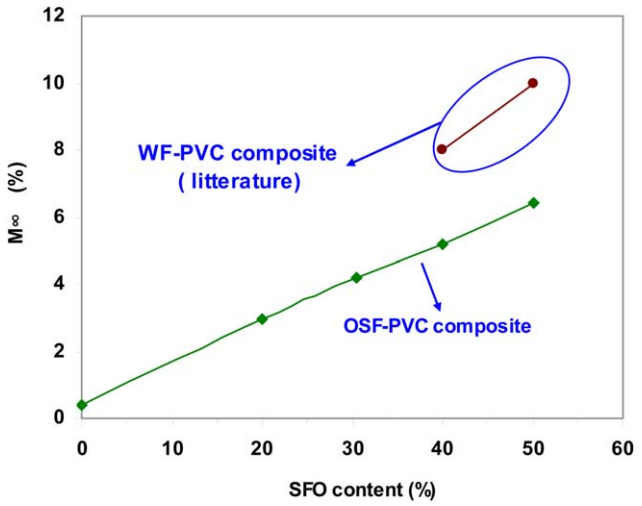

Figure 8. Plot of M_∞ versus filler loading for the coupled and uncoupled composite. [Color figure can be viewed in the online issue, which is available at wileyonlinelibrary.com.]

worth noting that compared to PVC-wood flour composites,[27] PVC-OSF composite exhibited a lower extent of water absorption. Indeed, at 40% and 50% wood flour loading, the equilibrium water absorption attained about 7% and 8%, respectively, which is 30% and 40% higher than that of PVC-OSF. The lower sensitivity of PVC-OSF-based composites to water absorption is likely associated with OSF ultratstructure. Actually, while the OSF particles are compact and exempt of any porosity (see MEB observation in Figure 2), the lignocellulosic fibers encompassed pores coming from the lumen and those trapped between the microfibrils in the cell wall, whose presence might constitute a locus for water accumulation. The lower cellulose content of the OSF compared to wood flour and lignocellulosic materials might be another possible reason likely to account for this behavior.

The evolution of the tensile mechanical properties of the OSF-PVC composite after immersion in water for 60 days to reach the adsorption equilibrium was also studied. Results given in Figure 9 revealed a fall in the tensile modulus and tensile strength by about 20% and 10%, respectively, after immersion in water. This decrease in the mechanical properties is quite expected and constitutes one of the shortcomings of lignocellulosic-based composite.[28] The debonding of the interfacial adhesion between the filler and the matrix following the water absorption, and the plasticization effect engendered by the water absorption by the lignocellulosic fillers are the main reasons accounting for this phenomenon.

Thermal Properties

Owing to the high sensitivity of PVC to thermal degradation and the possible alteration of this property in the presence of the lignocellulosic filler, the thermal stability of PVC-based composite is an important property worth to explore, especially that the resulting degradation often alters the color and the mechanical properties of the materials. To investigate the thermal stability of the PVC-OSF composite, the TGAs of PVC, OSF filler, and of the PVC-OSF composites under oxygen were carried out, and the results are given in Figure 10. The Derivative Thermogravimetry (DTG) curves (first derivative of the TGA) were also shown and the main degradation characteristics were collected in Table II.

The thermal degradation of OSF can be divided into three stages. Up to 200°C, about 7% weight loss is noted corresponding to the moisture departure, which is a common feature for lignocellulose fibers.[29] The initial thermal degradation of SFO started at 230°C and continued up to 300°C with a weight loss of about 60%. This stage is associated with the thermal degradation of hemicelluloses which are the most thermally sensitive components in the lignocellulosic filler.[18] The decomposition then continued with a third step occurring between 300 and 450°C with about 40% weight loss, assigned to the thermal decomposition of cellulose and lignin.[30] PVC was thermally stable up to a temperature of 240°C, and then started to degrade

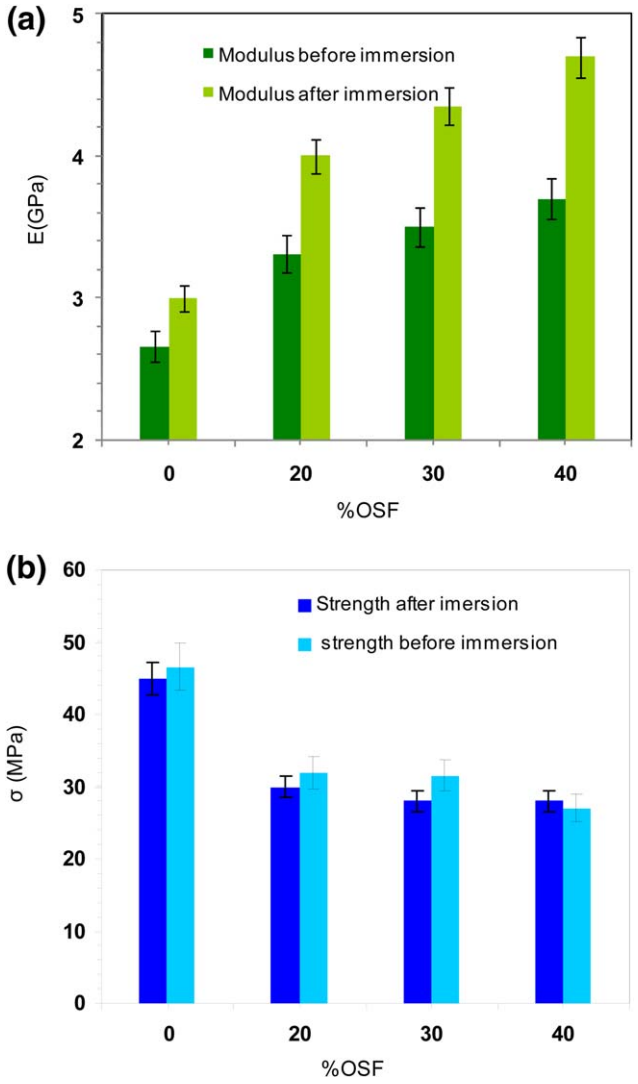

Figure 9. Evolution of the tensile modulus and tensile strength of PVC-OSF composite with different filler content after immersion for 60 days in water. [Color figure can be viewed in the online issue, which is available at wileyonlinelibrary.com.]

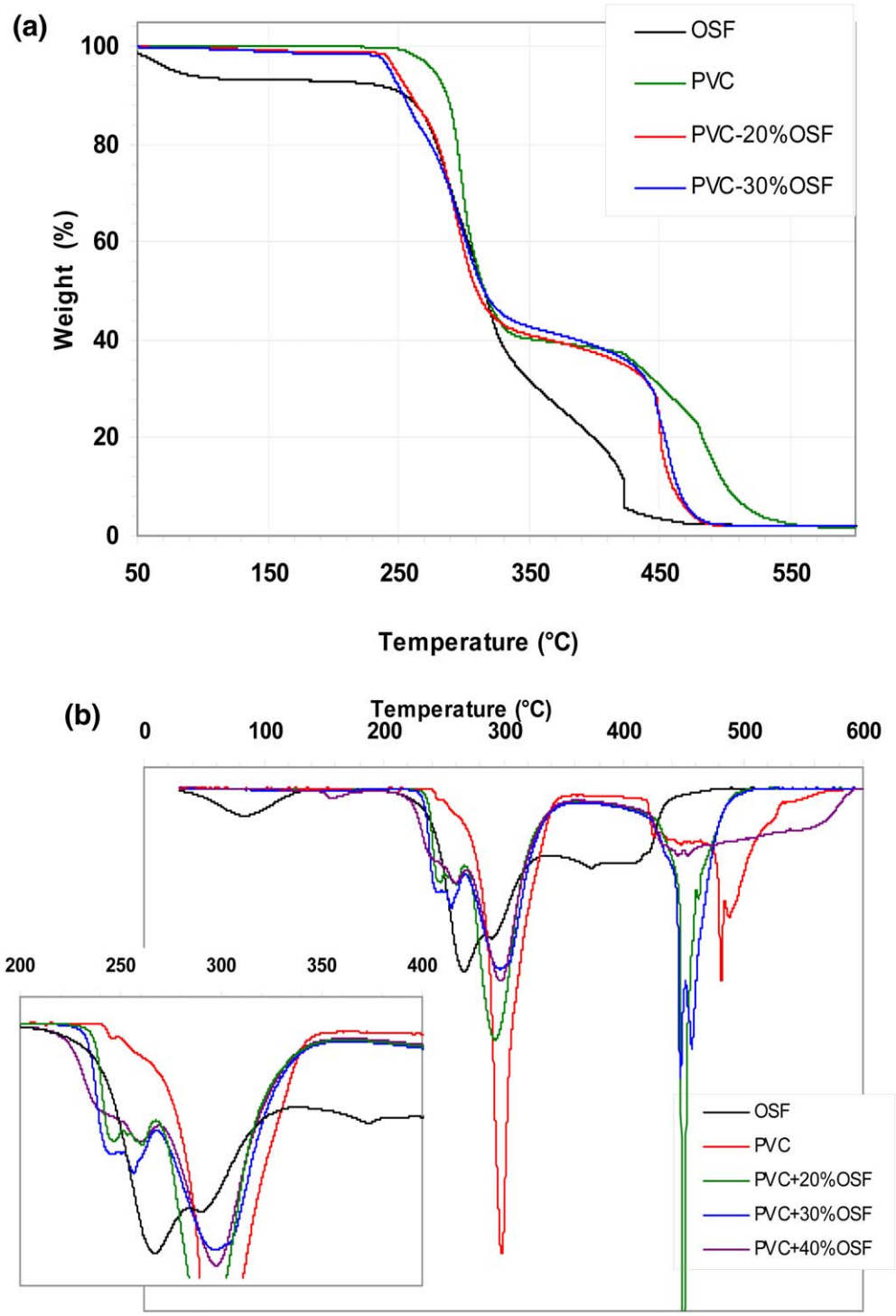

Figure 10. TG and DTG of PVC and composite with different OSF loading. [Color figure can be viewed in the online issue, which is available at wileyonlinelibrary.com.]

rapidly following two steps with maximum weight loss rates appearing at 290 and 480°C in the DTG curve. The first stage, involving a mass loss of about 60%, is attributed to the dehydrochlorination[23] of the PVC and the volatilization of the hydrogen chloride molecules (HCl). The second stage is much shorter than the first one and resulted from the thermal cracking of the carbonaceous conjugated polyene sequences generated by the dehydrochlorination.

Conversely, the TG of PVC-OSF exhibited a three-stage degradation process with maximum weight loss rates appearing at 240, 290, and 450°C in the DTG curve. The first step starting at about 220°C was not visible neither in the OSF nor in the PVC

Table II. Thermogravimetric Analysis Data Under Oxygen

		First stage			Second stage		
Samples	*T* onset/°C	Temperature range/°C	Tmax/°C	Mass loss (%)	Temperature range/°C	Tmax/°C	Mass loss (%)
OSF	211	30-136	60	7	211-287	267	85
PVC	233	233-344	299	60	412-512	482	36
PVC + 20% OSF	213	213-333	290	57	409-473	454	39
PVC + 30% OSF	205	205-332	286	56	407-473	452	38
PVC + 40% OSF	203	203-320	286	54	388-564	474	40

and increased in magnitude with the increase in the OSF content. This means that the incorporation of OSF reduces the degradation temperature of the material and accelerates the initial degradation of PVC matrix in the composite. This phenomenon was also observed in wood flour-PVC composite and was explained by the generation of formic acid during the degradation, whose presence accelerated the initial dehydrochlorination of the PVC. Given the quite similar chemical composition of OSF and wood flour, the same held for OSF filler. The second step in the thermal degradation of PVC-OSF composite occurred in the temperature range from 260 to 360°C. It resulted from the dehydrochlorination of PVC and the degradation of the hemicelluloses in OSF. The third stage started from 360 to 480°C is due to the carbonization process of the polymer.

The thermal properties of PVC-OSF composite loaded with different filler contents were also studied by DSC and the corresponding thermograms are given in Figure 11. All the thermograms show a well-defined Tg around 75°C with a position being insensitive to the filler content. At a higher temperature, a weak endothermic peak around 125°C is visible, which is most likely associated with the melting of the crystalline domains. Indeed, the PVC made commercially by radical polymerization has nearly random syndiotactic and isotactic sequences, which in turn limits the size of crystallizable syndiotactic sequences. Furthermore, the PVC powder exhibits three levels of substructure and is composed of grains irregular in shape with about 100–150 μm in diameter. Each grain consists of microparticles, with about 1–2 μm in diameter. The microparticles are in turn made up of smaller submicroparticles, approximately 10–30 nm in diameter, and exhibit 5–10% of crystallinity. The melting of the crystallite was reported to be in the range of from 115 up to 230°C.[25,31]

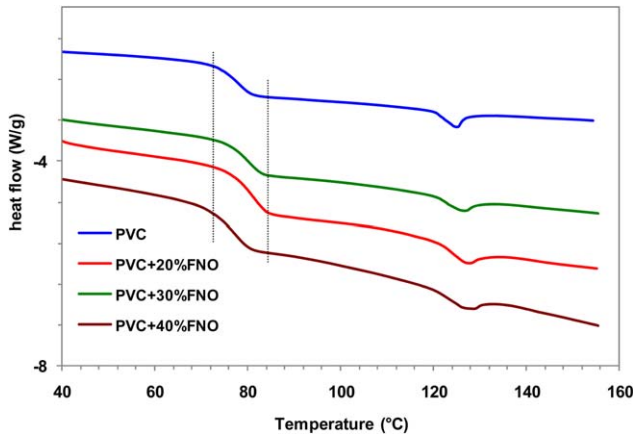

Figure 11. DSC thermogram of PVC and PVC-OSF composite with different filler content. [Color figure can be viewed in the online issue, which is available at wileyonlinelibrary.com.]

CONCLUSIONS

Composites based on PVC matrix and OSF were successfully prepared by melt compounding and injection molding. Among the benefits of the incorporation of OSF into the PVC matrix are the cost reduction and the valorization aspect in the field of material technology. Although the resulting PVC-OSF composites exhibited higher stiffness than PVC, the addition of OSF reduced the mechanical strength and the impact properties of the composite. For instance, at 40% filler loading, the tensile strength and the untouched Charpy impact strength were reduced by about 30% and 80%, respectively, compared to the unfilled matrix. This is in accordance with the results obtained when wood-based flour was used as filler in the PVC matrix. Based on the above investigation, the present PVC-OSF composite could be used in several applications, such as building and construction, the automotive industry, as well as in gardening and outdoor products.

ACKNOWLEDGMENTS

The authors would like to express their gratitude to "Ministère de l'enseignement supérieur et de la recherche scientifique de Tunisie," "Centre Technique de la Chimie- CTC," and OLEVARUM-Company for their financial support of this research through PNRI grant. Grateful acknowledgement is also addressed to Mrs. Joan Gandini for English revision.

REFERENCES

1. Akgun, N. A.; Doymaz, I. *J. Food Eng.* **2005**, *68*, 455.
2. Khraisha, Y. H.; Hamdan, M. A. *Energy Sources* **1999**, *21*, 319.
3. Baçaoui, A.; Yaacoubi, A.; Dahbi, A.; Bennouna, C.; Phan Tan Luu, R.; Maldonado-Hodar, F. J. *Carbon* **2001**, *39*, 425.

4. Wahby, A.; Abdelouahab-Reddam, Z.; El Mail, R.; Stitou, M.; Silvestre-Albero, J.; Sepúlveda-Escribano, A. *Adsorption* **2011**, *17*, 603.
5. Perinovic, S.; Andricic, B.; Erceg, M. *Thermochim. Acta* **2010**, *510*, 97.
6. Ayrilmis, N.; Buyuksari, U. *J. Mater. Sci.* **2010**, *45*, 1336.
7. Ihemouchen, C.; Djidjelli, H.; Boukerrou, A.; Fenouillot, F.; Barres, C. *J. Appl. Polym. Sci.* **2013**, *128*, 2224.
8. Papanicolaou, G. C.; Koutsomitopoulou, A. F.; Sfakianakis, A. *J. Appl. Polym. Sci.* **2012**, *124*, 67.
9. Ihamouchen, C.; Djidjelli, H.; Boukerrou, A.; Krim, S.; Kaci, M.; Martinez, J. *J. Appl. Polym. Sci.* **2012**, *123*, 1310.
10. Boukerrou, A.; Krim, S.; Djidjelli, H.; Ihamouchen, C.; Jua, M. J. *J. Appl. Polym. Sci.* **2011**, *122*, 1382.
11. Mousaab, A.; Heinric, G.; Wagenknecht, U. *Int. J. Polym. Mater. Polym. Biomater.* **2010**, *59*, 843.
12. Matosa, M.; Barreiro, M. F.; Gandini, A. *Ind. Crops Prod.* **2010**, *32*, 7.
13. López, J. P.; Boufi, S.; El Mansouri, N. E.; Mutjé, P.; Vilaseca, F. *Compos. B* **2012**, *43*, 3453.
14. Belhassena, R.; Boufi, S.; Vilaseca, F.; Lopez, J. P.; Mendez, J. A.; Francob, E. B. *Polym. Adv. Technol.* **2009**, *20*, 1068.
15. Djidjelli, H.; Benachour, D.; Boukerrou, A.; Zefouni, O.; Martinez-Véga, J.; Farenc, J. *Exp. Polym. Lett.* **2007**, *1*, 846.
16. Segal, L.; Creely, J. J.; Martin, A. E.; Conrad, C. M. *Text. Res. J.* **1959**, *29*, 786.
17. Bledzki A. K.; Gassan, J. *Prog. Polym. Sci.* **1999**, *24*, 221.
18. Iulianelli, G. C. V.; Maciel, P. M. C.; Tavares, M. I. B. *Macromol. Symp.* **2011**, *299*, 227.
19. Arbelaiz, A.; Fernandez, B.; Raunes, J. A.; Retegi, A.; Llano-Ponte, R.; Mondragon, I. *Compos. Sci. Technol.* **2005**, *65*, 1582.
20. Lulianelli, G. C. V.; Maciel, P. M. C.; Tavares, M. I. B. *Macromol. Symp.* **2011**, *299*, 227.
21. Abdelmouleh, M.; Boufi, S.; Belgacem, N.; Dufresne, A. *Compos. Sci. Technol.* **2007**, *67*, 1627.
22. Sun, X.; Lu, C.; Liu, Y.; Zhang, W.; Zhang, X. *Carbohydr. Polym.* **2014**, *101*, 642.
23. Frank, A.; Biederbick, K. Kunststoffkompendium; Vogel-Buchverlag: Wurzburg, **1984**.
24. Girones, J.; Mendez, J. A.; Boufi, S.; Vilaseca, F.; Mutje, P. *J. Appl. Polym. Sci.* **2007**, *103*, 3706.
25. Lin, Q.; Zhou, X.; Dai, G. *J. Appl. Polym. Sci.* **2002**, *85*, 2824.
26. Gasparovic, L.; Korenova, Z.; Jelemensky, L. *Chem. Pap.* **2010**, *64*, 174.
27. Müller, M.; Radovanovic, I.; Gruneberg, T.; Militz, H.; Krause, J. *Appl. Polym. Sci.* **2012**, *125*, 308.
28. Joseph, P. V.; Rabello, M. S.; Mattoso, L. H. C.; Joseph, K.; Thomas, S. *Compos. Sci. Technol.* **2002**, *62*, 1357.
29. Sebio-Punal, T.; Naya, S.; Lopez-Beceiro, J.; Tarrıo-Saavedra, J.; Artiaga, R. *Therm. Anal. Calorim.* **2012**, *109*, 1163.
30. McNeill, I.; Memetea, L.; Cole, W. *Polym. Degrad. Stab.* **1995**, *49*, 181.
31. Fillot, L. A.; Hajji, P.; Gauthier, C.; Karina, M. V. *J. Vinyl Addit. Technol.* **2006**, *12*, 98.